12-2020

Comparison of Additively Manufactured and Wrought 17-4 PH Stainless Steels in Ultra Low Cycle Fatigue

Timothy Strasser
University of Arkansas, Fayetteville

Comparison of Additively Manufactured and Wrought 17-4 PH Stainless Steels in Ultra Low Cycle Fatigue

A thesis submitted in partial fulfillment
of the requirements for the degree of
Master of Science in Civil Engineering

by

Timothy Strasser
Harding University
Bachelor of Science in Mechanical Engineering, 2019

December 2020
University of Arkansas

This thesis is approved for recommendation to the Graduate Council.

_____
Gary S. Prinz, Ph.D.
Thesis Director

_____
Cameron Murray Ph.D.
Committee Member

_____
Micah Hale Ph.D.
Committee Member

Abstract

Additive manufacturing (AM) processes allow for creation of complex geometries that are otherwise impractical to fabricate with traditional subtractive methods. AM technology has potential to improve the optimization of seismic lateral force resisting components which dissipate seismic energy through large plastic strains; however, the ultra low-cycle fatigue performance of AM metals are not yet well understood. Void formation during the AM fabrication process has potential to affect performance. This study compares the performance of heat-treated and non-heat-treated AM and wrought 17-4PH stainless steel in Ultra Low Cycle Fatigue. To understand ULCF performance differences between the AM and wrought specimens, post fracture microstructure, fractography, surface hardness, and material characterizations are conducted. Results indicate reduced fatigue life for AM 17-4PH stainless steel as compared to the wrought counterparts. Fatigue life reductions of 62% and 65% were measured for the AM steel materials (as compared to the wrought counterparts) at 3% and 4% applied strain amplitude respectively. Applied material heat treatments had no observable effect on ULCF performance.

Acknowledgements

First and foremost I thank God, without him nothing is possible. I would like to thank my wife, Callie, who has shown unwavering support throughout my academic journey, I love you. Thank you to my parents, Fred and Rebecca Strasser who instilled a work ethic and a desire to glorify God in the way that I work and live before others. I am grateful to my brother, Matthew N. Strasser, who first encouraged me to explore engineering and now serves as a mentor. Thank you Dr. Gary Prinz, for investing in me and diligently contributing to my growth as an engineer and professional. Thank you to Dr. Micah Hale and Dr. Cameron Murray for your valuable critiques that have made this thesis the best it can be. Thank you David Gonzalez-Nino for your mentorship during our work together. Thank you Mr. David Peachee, and Mr. Mark Kuss who were instrumental in the overall success of this project.

This material is based upon work supported by the National Science Foundation under Grant No. 1751699. Kind support of AM material specimens provided by the National Institute of Standards and Technology (NIST) is also acknowledged and greatly appreciated.

Table of Contents

List of Figures

List of Tables

1. Introduction

1.1 Overview

Additive manufacturing (AM) provides a novel approach to optimize designs and decrease waste, making it an attractive alternative to traditional subtractive processes. Earthquake engineering can see a notable improvement by applying this technology to the optimization of yielding seismic dampers (YSD) such as that shown in **Figure 1**.

Figure 1. School building outfitted with YSD [1].

YSD are passive devices that reduce second order effects on a building through plastic deformation as shown in **Figure 2**. The function of the YSD is to plastically deform, thus dissipating seismic energy.

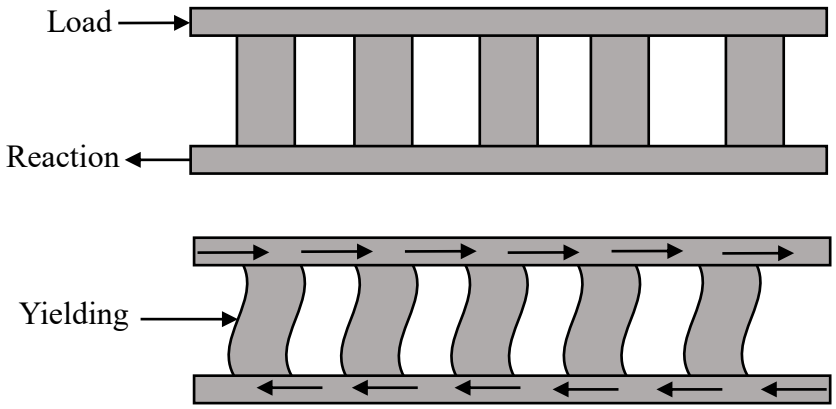

Figure 2 Yielding Seismic Damper dissipating energy via. plastic deformation

The production of metallic parts via AM is a relatively new process and the behavior of materials produced through AM processes is still in question [2, 3, 4, 5]. Comprehensive mechanical and fatigue studies are needed before AM materials can replace traditionally cast components [3]. Austenitic stainless steels are ideal for AM parts due to their weldability, microstructure, and high impact strength [2]. This study investigates the ultra low cycle fatigue (ULCF) performance of additively manufactured17-4 PH stainless steel and compares the results to traditionally produced wrought specimens. Future work will conduct ULCF tests on micro-scale specimens taken from unstrained portions of the macro-scale specimens to evaluate the significance of microscopic defects on the ULCF performance of the material. Microscale test results will be compared with the macroscale material results generated in this study to develop strain-life curves to predict material performance.

2. Review of relevant literature

2.1 Selective Laser Melting process

Additive manufacturing is considered by ASTM as, “A process of joining materials to make objects from 3D model data, usually layer upon layer, as opposed to subtractive

manufacturing methodologies" [6]. Currently, the most popular method of AM is a subset of Powder-Bed Fusion-Laser, known as Selective Laser Melting (SLM) [7]. The SLM process is depicted in **Figure 3**. During SLM process, metallic powder is rolled over the surface of the substrate where a laser melts the powder in a particular region based on a discretized model defined in computer assisted design (CAD) software. Process parameters can be adjusted to achieve slower or faster cooling rates as well as melt pool size and laser penetration depth [7]. Due to the layered process, components produced via SLM exhibit anisotropic microstructure and behavior based on their build orientation (see **Figure 4)**.

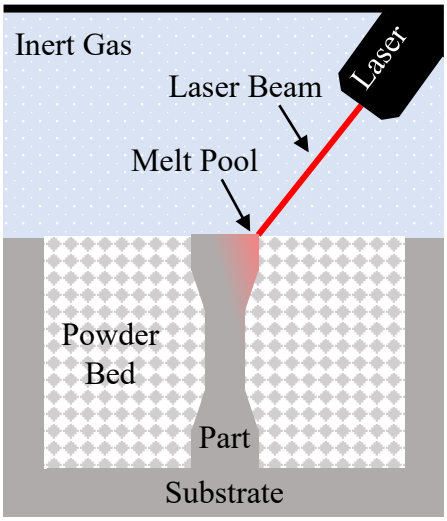

Figure 3. SLM process

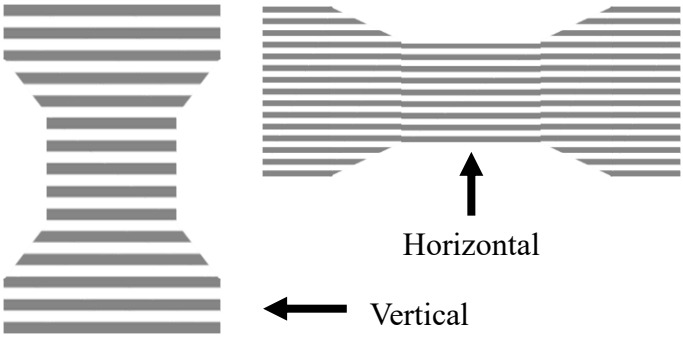

Figure 4. Vertical and Horizontal build orientations

2.2 Comparison of mechanical performance

The strength of AM 17-4 PH materials have been shown to be equivalent or better than traditional wrought materials, when built in the horizontal position (parallel to the direction of loading) [2, 7, 8]. AM steel parts have exhibited equivalent performance to traditional steels in certain instances of fatigue, which has been attributed to finer grain structures due to the powder-melting process [9]; however, several research studies [7, 10, 11, 12] achieved tensile yield strengths that are much lower than those of wrought materials. It is important to note that the mechanical properties of AM materials depend primarily on their microstructure, a byproduct of the thermal history during manufacturing [12].

2.3 Effects of thermal history on phase composition

Steels produced via SLM tend to experience rapid cooling when built in a horizontal orientation due to a small portion of the material being melted at each pass thus, allowing rapid cooling before the next pass. Rapid cooling acts like quenching which induces a higher martensite content in horizontal specimens [2, 10]. By contrast, vertically built specimens exhibit a slower cooling rate because less time passes before the next layer is melted, leading to a quasi-annealing process and higher austenite content [2].

Phase directly affects microhardness [10, 12]. Research in [2, 3] suggested that a post-manufacturing heat treatment of AM steels may be necessary to achieve tensile strengths similar to wrought counterparts due to the discrepancy in cooling during AM processes, which decreases material hardness and yield strength [7].

2.4 Effects of heat treatment

Research by [2] observed heat-treated specimens outperforming as- built counterparts in LCF but underperformed as-built counterparts in HCF; however, other research in [5] noted the

effect of heat treatment on fatigue life depends entirely on the strengthening mechanism of a given steel. Because the effects of heat treatment are different for every steel, and there is no clear trend for its effect on the fatigue life of 17-4 PH, it is difficult to determine the effects of post-fabrication heat treatments as it may pertain to the performance of 17-4 PH in ULCF.

2.5 Comparison of tensile properties

Research by [3, 10, 11] noticed that AM parts have finer microstructures, which [10] correlated with higher ultimate tensile strengths but not yield strength, when built in the horizontal position. Research by [10] further suggests that ultimate tensile strength is correlated with decreased elongation to failure, therefore AM materials are said to exhibit less ductility than conventional wrought materials. It is important to consider the physical demands on the material before conducting any post-fabrication heat treatments, as retained austenite has a positive effect on the ductility of the material but has a detrimental effect on resistance to fatigue-induced wear [13].

2.6 Effect of voids

The greatest concern of implementing AM parts in civil infrastructure components is the inherent defects, particularly voids that form in the material as a result of the additive process. Voids induce stress concentrations during mechanical loading based on their size, shape, and location relative to the surface [2]. Various studies ([2, 7, 3]), have agreed on two types of voids: spherical and slit-shaped. Spherically shaped pores are attributed to gas entrapment; whereas, oval or slit-shaped pores are attributed to unmelted particles during the manufacturing process. Slit-shaped voids are particularly detrimental if they lie normal to the direction of loading due to a large reduction in cross sectional area as shown in **Figure 5**.

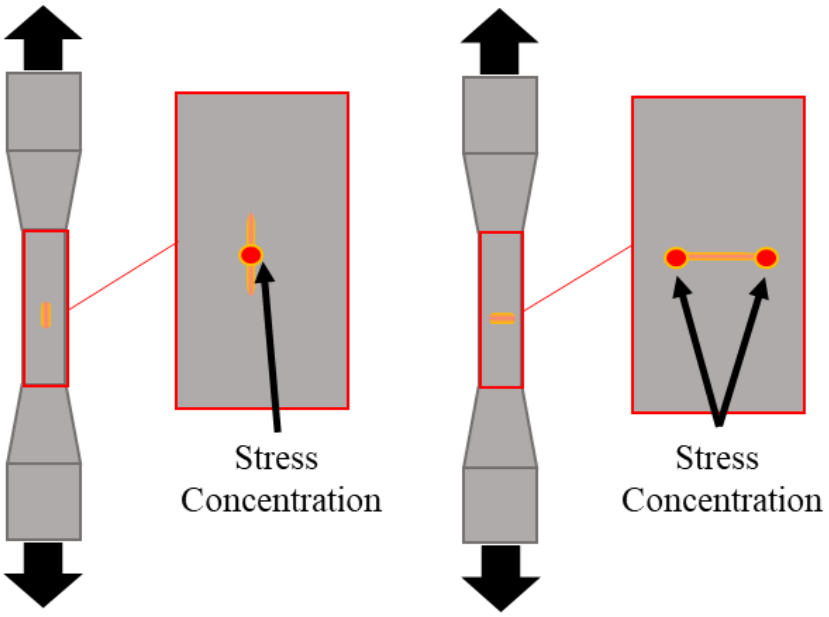

Figure 5. Stress concentrations based on void orientation

Currently, there is no cost-effective way to reduce the size of these pores, and although heat treatment can increase tensile yield, ultimate strength, or ductility of AM parts, it cannot reduce porosity [2, 12]. Because the mechanical properties of AM 17-4 PH produced by SLM have been well-studied, this study will also focus on material performance in ultra low-cycle fatigue.

2.7 Introduction of fatigue

Fatigue is the primary cause of structural failure and may be described as repeated stresses and strains that induce failure below the ultimate tensile strength due to microstructural evolutions [14]. Because fatigue is a localized phenomenon, failure is typically caused by stress concentrations that form due to imperfections on or beneath the surface of the material; however, in ultra low-cycle fatigue, post yield void growth and coalescence due to repeated plastic strain cycles leads to macro-fracture and ultimate failure. The effect of internal fabrication flaws on material performance is dependent on the strain amplitude rather than stress-concentration driven brittle fracture. Large plastic deformations are more damaging in ULCF [4].

2.8 Fatigue regimes

Fatigue may be categorized into three regimes: High Cycle Fatigue (HCF), Low Cycle Fatigue (LCF), and Ultra Low Cycle Fatigue (ULCF) as shown in **Figure 6**. High Cycle Fatigue represents cycles-to-failure counts in excess of one million and has been thoroughly investigated, and a reasonable approximation method exists known as Basquin's equation [15]. Low Cycle Fatigue is characterized by a cycle-to-failure count greater than one hundred but not in excess of one million, and a reasonable approximation method for this regime exists, known as Coffin-Manson equations [16]. Ultra-Low Cycle Fatigue is characterized by cycles-to-failure counts less than one hundred, and there is no accepted ULCF life prediction model at this time [14]. The discrepancy exists, primarily, for two reasons: 1) ULCF consists of large plastic deformations that have not been as useful to mechanical and aerospace research in the past, and 2) inelastic deformations complicate conventional LEFM or EPFM techniques that correlate "far-field" stresses with stresses near a crack tip [4].

Ultra Low (ULCF)	Low (LCF)	High (HCF)
100 > N	1M > N > 100	N > 1M

Figure 6. Fatigue spectrum

2.9 Previous attempts to model ULCF

Attempts to modify previous elastic-based theories to account for plastic deformation do not consider the change in failure mode from fatigue cracking to ductility exhaustion or the the change in microstructural behavior [14]. [17] sought to connect tensile strength with ULCF performance through the common ductility exhaustion failure mode. [18] agreed with [17] but also suggested that ULCF mechanisms include microvoid distortion during cyclic loading which

alters internal stress concentrations with each cycle, and [14] agreed with this claim and pointed out that microvoid dialation/elongation is the most important micro-damage mechanism in metals subjected to ULCF. Because AM steels tend to contain many more internal flaws than wrought counterparts, it is reasonable to assume that their performance in ULCF may be compromised. Additionally, thermal gradients and subsequent machining can affect the microstructure and residual stresses at the surface, both of which can prove detrimental to fatigue behavior [5]. However, steels with a metastable austenitic microstructure (like 17-4 PH) exhibit strain-induced transformation from austenite to martensite (known as strain hardening) that, in some cases, may be enough to offset the negative effects of internal microvoids [2]. Despite these observations, no models consider all these variables when predicting ULCF behavior.

2.10 Need for empirical approach

Due to the lack of models or material-based trends available at this time, the ULCF performance of AM 17-4 PH stainless steel compared to wrought counterparts will be determined empirically. Results will be processed using a strain-based approach for a comprehensive analysis of the plastic region during testing [7]. Future work can attempt to model material behavior based on empirical data from this study.

3. Experimental procedure

3.1 Sample fabrication

Samples were fabricated according to the dimensions shown in **Figure 7**. AM specimens were fabricated by the National Institute of Standards and Technology (NIST) via EOSINT M270 DMLS via. Selective Laser Melting (SLM). Rectangular specimens were constructed in the horizontal direction to obtain the best mechanical properties [5]. AM samples were

constructed in a rectangular shape rather than the final form to ensure that the surface finish due to machining were comparable to wrought (W) counterparts.

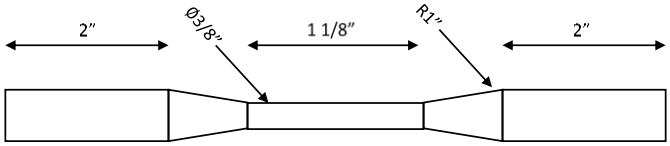

Figure 7. Specimen dimensions

Half of the AM samples were subject to a heat treatment suggested by the EOS company (known as a stress relieving (SR) heat treatment) at 650º C for one hour, in order to shift their primary phase composition from austenite to martensite. The other AM samples were left as-built (AB). Wrought specimens were fabricated from rectangular pieces of ASTM-compliant, hot rolled 17-4 PH stainless steel (Condition A). Half of the wrought specimens underwent heat treatment (HT) at 650º C for four hours to shift some of the martensite phase to austenite. The other wrought specimens were left in the As Rolled (AR) condition. The material composition of the wrought and AM specimens is listed in **Table 1**, and both sample types are within the composition limits of the other.

Table 1. Material composition of wrought and AM steel provided by manufacturers

Element	%C	%Si	%Mn	%Cr	%Ni	%Cu	%Mo	%Nb
Wrought	0.031	0.314	0.876	15.10	4.30	3.310	0.083	0.190
AM	< 0.07	< 1	< 1	15-17.5	3-5	3-5	< 0.5	0.15 -0.45

3.2 Testing procedure

Strain-controlled tensile and Ultra-low cycle fatigue tests were conducted in accordance with [19] using a Walter + Bai Ag Servohydraulic Biaxial fatigue testing machine. Fully reversed (R= -1), strain controlled, uni-axial cyclic loading was conducted at 2%, 3%, and 4% strain amplitude. The fatigue deformation history of a sample undergoing 4% strain is shown in **Figure 8**.

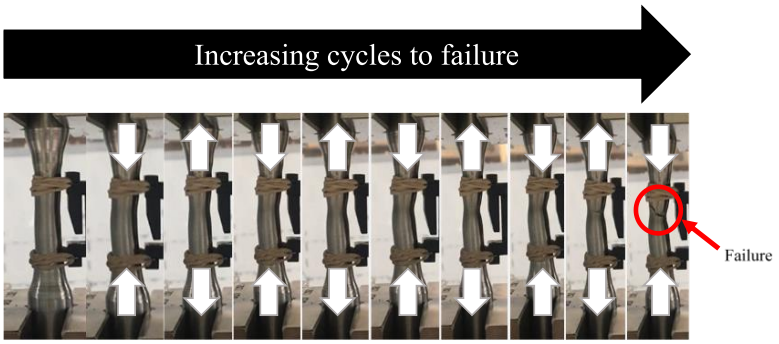

Figure 8. Fatigue sequence at 4% strain

An MTS knife-blade extensometer was fixed to the gage of each fatigue specimen (shown in **Figure 9**) to measure specimen strains during loading. The number of constant amplitude applied fatigue cycles were recorded until failure. Fracture surface features of the tensile and fatigue specimens was photographed post-failure using scanning electron microscopy.

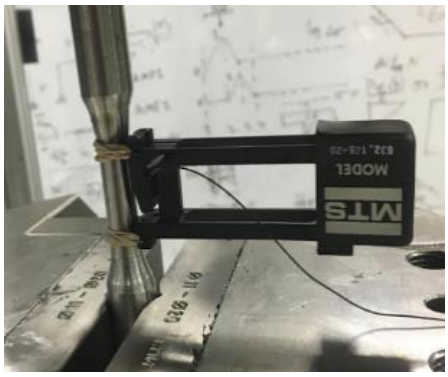

Figure 9. MTS knife blade extensometer fixed to specimen

3.3 Material characterization

Photographs of the fracture surfaces were conducted with a Tescan Vega 3 scanning electron microscope (SEM). Additionally, phase composition was studied through x ray diffraction (XRD) analysis and Vickers Hardness tests. Prior to XRD analysis or hardness testing, a plug of steel was taken from the grip and gage sections, shown in **Figure 10**.

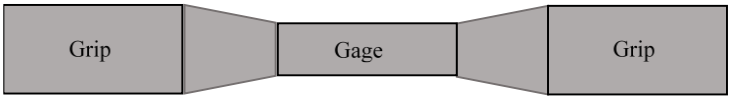

Figure 10. Grip and gage regions of the sample

Phase composition measurements of the gage section are limited to the area where necking did not ocurr, due to the dificulty in measuring this region [12]. Specimens were mounted using a BUEHLER SIMPLIMET 4000, and the surface of the specimen was polished down to one micron using a METASERV 2000 polisher. XRD measurements were conducted using a PANalytical X'Per MRD diffractometer which used Cu $K_{\alpha 1}$ radiation (λ=1.540598 Å) at an operating voltage and current of 45kV and 40mA, respectively. Hardness tests were conducted with a Pace Technologies' model HV-1000 microhardness indenter, using a load of 100-gf and a dwell time of 15 seconds. The devices mentioned are shown in **Figure 11.**

Figure 11. BUEHLER SIMPLIMET 4000, PANalytical X'Per MRD, METASERV 2000, and Pace Technologies' model HV-1000, respectively

4. Results and discussion

4.1 XRD Results

Figure 12 shows XRD results for the given spectra. The W-AR grip was completely martensitic. Heat treating the wrought steel shifted a small portion of the matrial phase in the grip from martensite to austenite. The AM-AB grip contained slightly more austenite than

martensite, which concides with [13] who noted near-equal amounts of austenite and martensite in the as-built condition. Heat treating the AM steel shifted the primary phase from austenite to martensite.

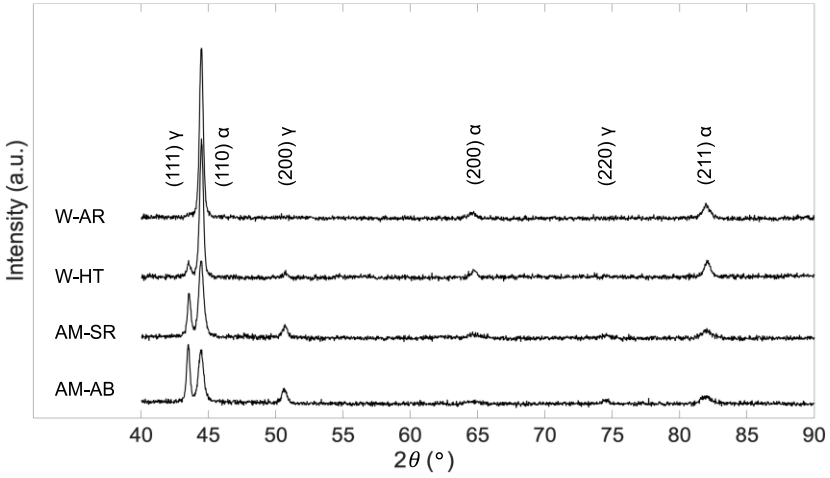

Figure 12. XRD readings for the four specimens prior to mechanical testing

4.2 Tensile Test Results

Table 2 compares the results of displacement controlled tensile tests obtained from **Figure 13**. In Table 2 and Figure 13, W-HT specimens exhibited slightly lower yield and ultimate strength(s) compared to W-AR, which can be attributed to trace amounts of austenite that formed due to heat treatment. Wrought specimens were identical in ductility, both rupturing at 15.5%. AM specimens exhibited lower yield strengths than wrought counterparts (600 MPa compared to 900 MPa) which can be attributed to a higher austenite content in the AM specimens. AM-AB, W-AR, and W-HT were similar in ultimate strength (1050 MPa), whereas AM-SR reached an ultimate strenth 1.5 times that observed in other specimens (1500 MPa).

Table 2. Strain, yield, and ultimate tensile values for all four specimen categories

	Actual Yield (MPa)	Actual Ultimate (MPa)
W-AR	928	1060
W-HT	892	1012
AM-AB	651	1071
AM-SR	538	1502

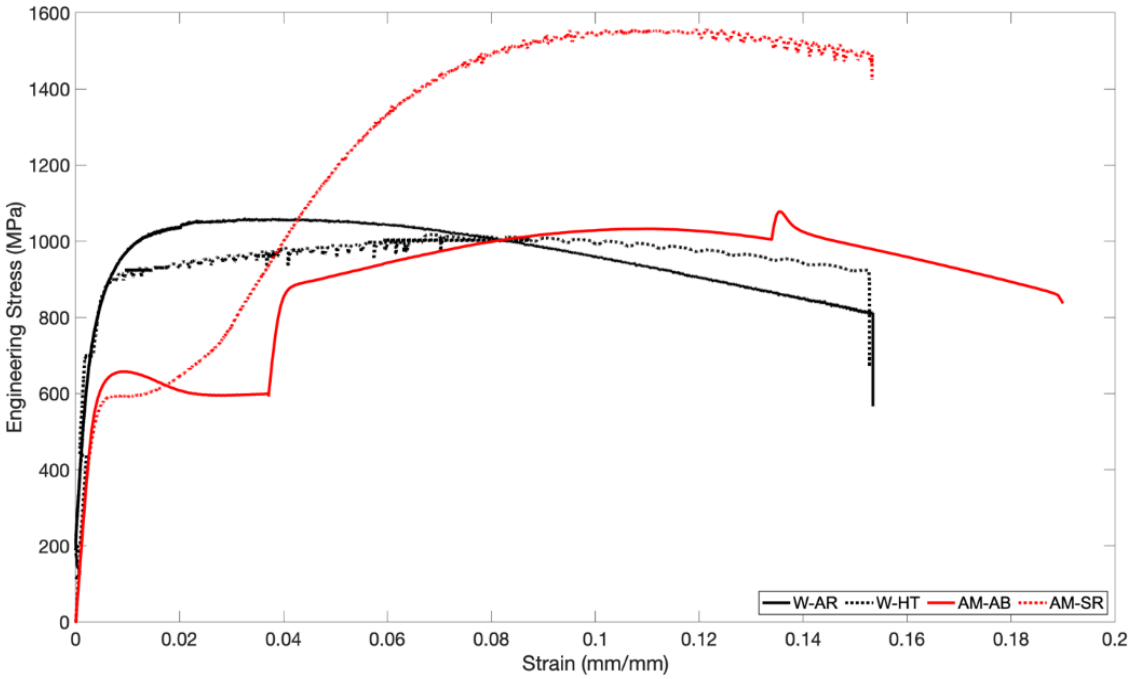

Figure 13. Displacement controlled tensile test results

The tensile test for AM-AB does not follow a characteristic shape, this is due to a momentary pause in testing. This pause is not believed to have comprimised critical data values (yield, ultimate strength, and elongation to failure).

Results are also presented in **Figure 14** to allow further visual observation. AM-AB exhibited more ductility than the other three sample types which can be attributed to its increased austenite content.

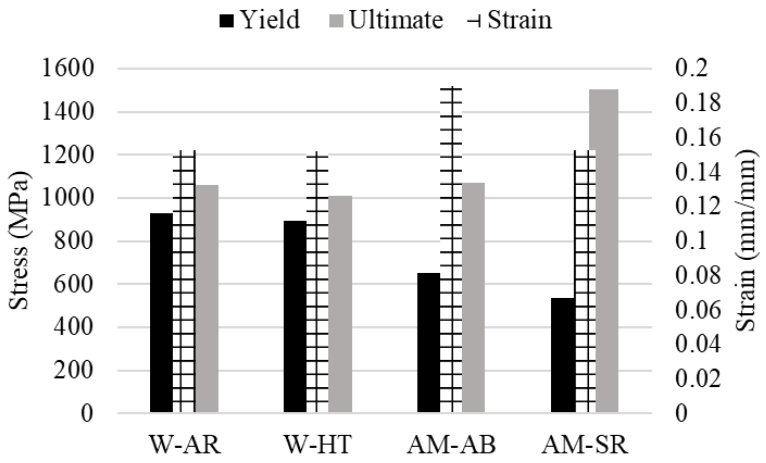

Figure 14. Comparison of expected tensile values and results obtained in this study

W-AR specimens performed as expected, whereas W-HT specimens exhibited lower yield and ultimate strength than expected. This difference is likely due to differences during the heat treatment process. AM -AB performed better than expected, and AM-SR slightly underperfomred in yield but exceeded expectations in ultimate strength.

4.3 Effect of heat treatment on tensile results

Heat treatment had little effect on the tensile performance of wrought 17-4 PH. It is important to note: the wrought steel, in both conditions, was primarily martensite; whereas, AM-AB steel was primarily austenite which enabled the AM steel to undergo large amounts of strain-induced hardening due to austenite to martensite transformation [5]. The phase composition of AM steels is not identical in wrought steels. An explanation for this is: finer grain structures of AM steels developed (as a result of the additive process) enable higher ultimate strengths, at lower martensite compositions, than wrought counterparts [7, 10]. This may explain how AM-SR exhibited a 1.5 increase in ultimate strength over the AB counterpart. SR treatment changed the composition from primarily austenite, to primarily marensite; therefore, the ultimate tensile strength should increase. The predominately martensitic AM specimen achieved signifcantly

higher ultimate strengths than the as-built counterpart. This indicates strain-hardening is not the governing factor of ultimate tensile strength. The AM-AB specimen may have experienced more strain hardening due to a higher austenite content; however, the results show that a more martensitic AM exhibited a higher ultimate strength than as-built counterparts. Therefore, wrought 17-4 PH is inferior to AM counterparts for this function.

AM-SR and both wrought conditions were similar in ductility. AM-AB is approximately 20% more ductile than wrought or AM-SR which aligns with [11] but contrasts with [2], which claimed that internal pororsity would decrease elongation to failure of the material. Greater elongation to failure is attributed to higher amounts of austenite in the AM-AB specimen than the AM-SR specimen. Heat treatment of wrought steels had no effect on the elongation to failure, indicating that the specimens were predominately martensitic.

4.4 Hardness test results

Hardness values are partially attributed to the material phase composition. Higher hardness values in a given material indicate greater amounts of martensite in the piece of material [10]. Results from Vicker's hardness tests from this study compared to [13] in **Table 3** and

Figure 15

Table 3. Hardness values in strained and unstrained sections

	Grip Hardness	Gage Hardness	% Change
W-AR	335	356	+6
W-HT	356	333	-7
AM-AB	294	475	+38
AM-SR	432	535	+19

AM-AB experienced more strain hardening than AM-SR, suggesting that AM-AB has a higher austenite content than AM-SR which supports the disussion of the tensile test results. AM samples exhibit higher amounts of strain-hardening than wrought samples, due to a higher austenite content prior to mechanical testing. Wrought steels exhibited low amounts of strain hardening, suggesting that the wrought steel was predominately martensitic (i.e. Condition A) prior to mechanical testing.

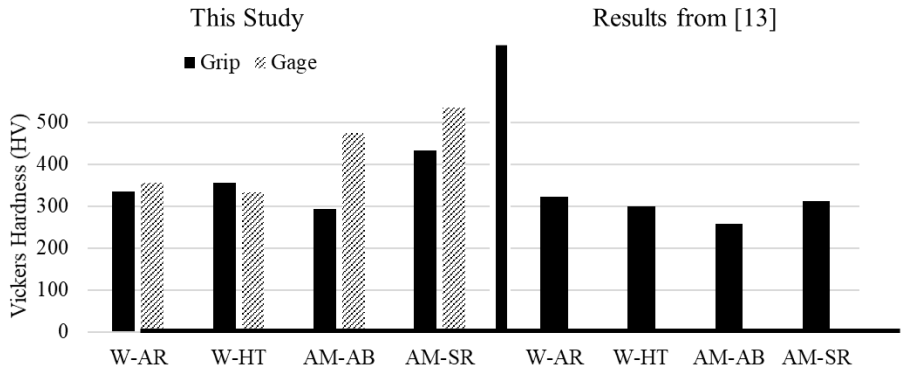

Figure 15. Hardness values before and after testing from this study and hardness values before testing from [13].

One anomaly observed during hardness testing is the decreased hardness from the grip to the gage secion of the heat treated wrought sample which is believed to be the result of polishing the grip section for an extended period of time, inadverntly shifting the phase composition on the surface to a higher martensite content than the gage section [12].

4.5 Microstructure

Images for wrought and AM steel and are shown in **Figure 16**. Observable change ocurred between wrought and AM materials due to theire respective heat treatments. Heat treated wrought steel appears to have a finer microstructure. Heat treated AM specimens do not appear different from as-built counterparts.

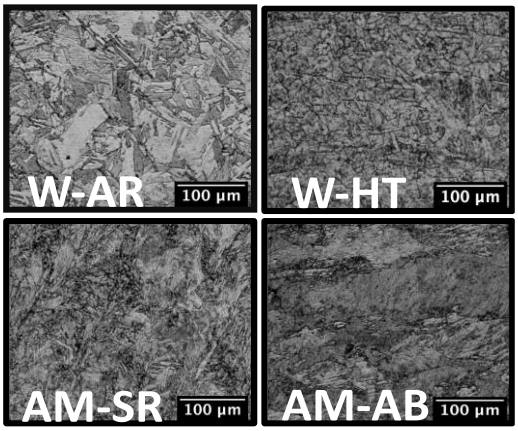

Figure 16. Microstructure of each specimen type prior to mechanical testing

4.6 ULCF test results

Results of ULCF data are recorded in **Table 4** and plotted in **Figure 17**. Heat treatment had no effect on the performance of AM 17-4 PH in LCF (which contrasts [2]) or ULCF. AM 17-4 PH performed similarly to wrought counterparts in LCF; however, wrought steel outperformed AM steel by >20 cycles in ULCF.

Table 4. ULCF results for this study

Strain (%)	W-AR (cycles)	W-HT (cycles)	AM-AB (cycles)	AM-SR (cycles)
2	384	575	515	462
	337	471	-	-
3	79	118	47	44
	105	151	-	37
4	35	41	14	14
	50	32	15	12

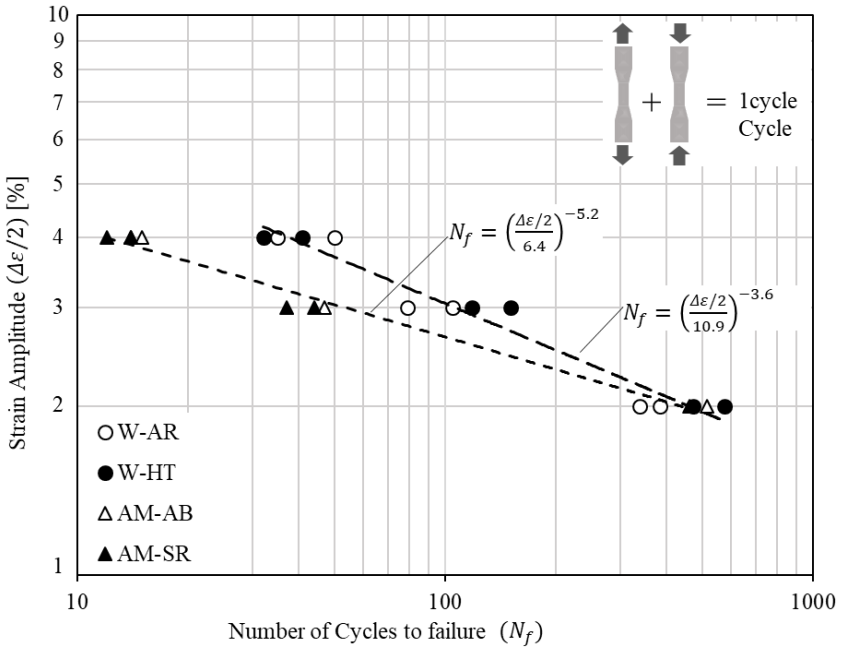

Figure 17. Results of ULCF testing for AM and wrought counterparts in both conditions

Multiple studies have attributed the lesser fatigue peformance of AM steels to the presence of voids due to umelted particles and/or gas entrapment during the manufacturing process. These voids act as stress concentrations and their influence on fatigue life results from their size and shape. Due to the localized phenomenon of fatiuge, fewer amounts of large voids is more detrimental than large amounts of smaller voids [2]. Literature suggests retained austenite is beneficial in some fatigue applications because it slows crack propagation during plastic straining [11]. Because strain-induced transformation from austenite to martensite increases with larger plastic strain amplitude [2], it would have been reasonable to assume that the ULCF beahvior of AM steels would be greater due to their increased austenite content; however, ULCF results demonstrate that, like tensile strength, the capacity of a material to undergo strain hardening is not the determining factor of how well it will perform.; instead, size and shape of internal pores is assumed to be the most significant aspect of material performance in this

regime. At this point, it is convenient to investigate the fracture surface of the ULCF specimens to evaluate if large pores were present and whether they acted as nucleation sites for fracture.

4.7 Fractography

The fracture surface of an AM and wrought specimen (both tested at 4% strain) are shown in **Figure 18** and **Figure 19**, respectively. The wrought surface is covered in spherical dimples, characteristic of ductile fracture [2, 3]. Failure in wrought specimens is attributed to non-metallic inclusions, which initiated crack formation.

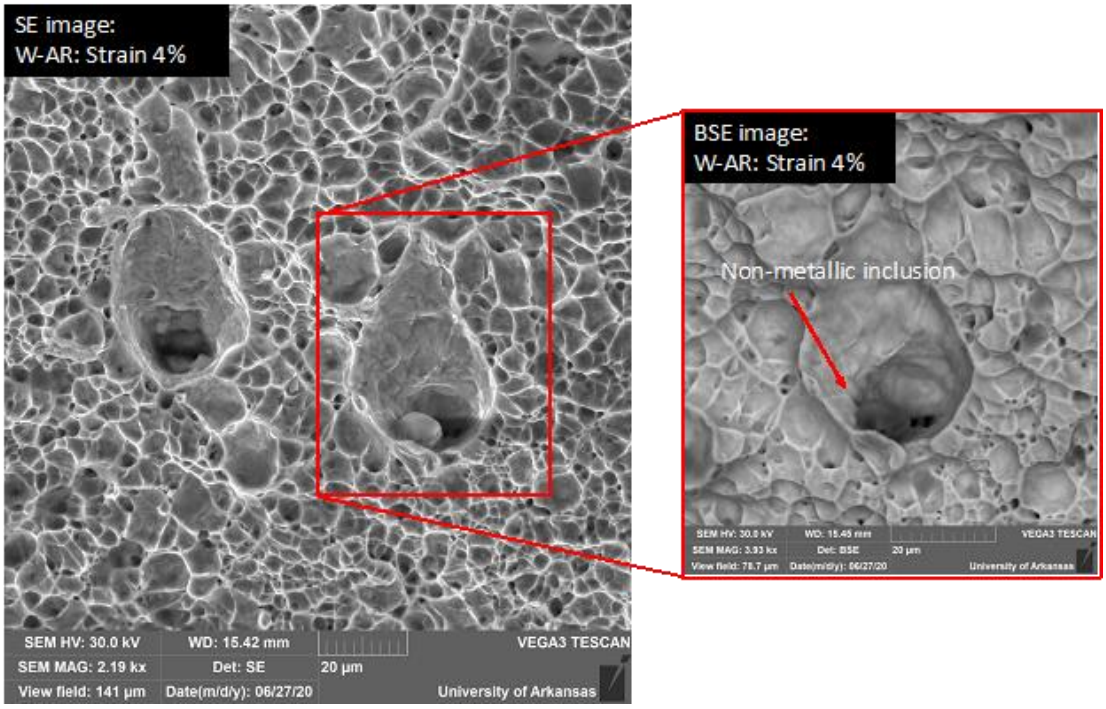

Figure 18. Fracture surface of wrought specimen subjected to ULCF at 4% strain

The surface of the AM specimen is covered in asperities, typical of brittle fracture. Failure in AM specimens is attributed to internal pores that formed as a result of unmelted particles and gas entrapment, as shown in **Figure 19**.

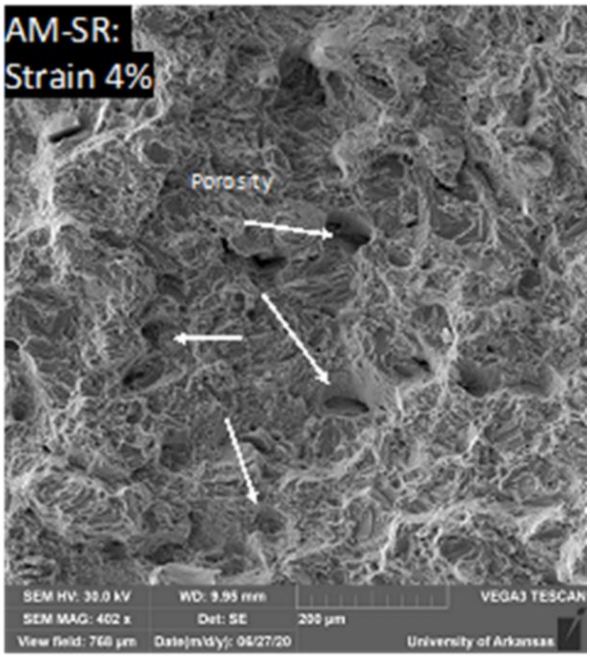

Figure 19. Fracture surface of the AM specimen subjected to ULCF at 4% strain

The fracture surfaces of AM tensile specimens are depicted in **Figure 20**. Voids in the AM steel were found to be up to 200 μm in diameter whereas, voids in the wrought steel were around 30 μm in diameter. The size and shape of voids in the AM metal confirm that they are the likely agent for the reduced fatigue life, which is also supported by [2]. Slit-shaped pores like the one shown in **Figure 20** is considered to be the initiation site, after which large plastic strains caused the cracks to grow and necking to occur in the surrounding areas until crack coalescence induced failure. The dimples on the fracture surface of the tensile specimen are deeper than those

on the fatigued samples. This difference is due to a higher “critical void ratio” [4].

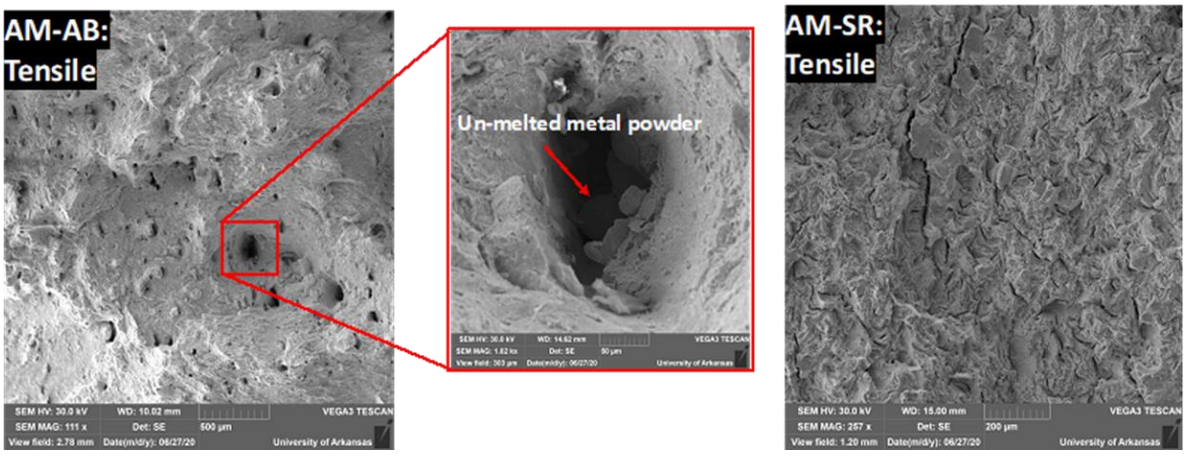

Figure 20. Tensile test fracture surface for AM 17-4 PH in both conditions

4.8 General conclusions of test results

AM specimens subjected to a stress-relieving heat treatment demonstrated improved ultimate tensile strength and hardness. The austenite-inducing heat treatment did not affect tensile values for wrought steel. AM 17-4 PH failed at fewer cycles than wrought steel in ULCF which is attributed to pores inherent to the AM material. Heat treatment has a negligible effect on the ULCF performance of both AM and wrought 17-4 PH. Because there is currently no cost-effective way to reduce porosity, designers should not assume AM 17-4 PH stainless steel performs the same as wrought counterparts in ULCF.

5. Future work based on this study

5.1 Issues with modifications to previous models

Design limits specified in AISC and AASHTO ensure that engineers design within a material’s elastic limit, which allows engineers and design software to employ linear elastic fracture mechanics (LEFM) for fatigue that is induced by relatively small displacements.

However, large plastic deformations during ULCF invalidate the methodology of LEFM [4]. [20] developed modified Coffin-Manson equations that present reasonable approximations of the loading mechanism by focusing on the effects of external factors on component stability [21] but a material can also cause instabilities, due to intrinsic defects and discontinuities [15]. Furthermore, this model lacks a microstructural basis [14]. ULCF differs from LCF in part, due to failure mode. As the strain range increases, the number of required reversals to failure decreases; this phenomenon is attributed to a transition from crack propagation to ductility exhaustion, akin to this is the nucleation site for the failure [17]. In fact, the nature of the applied loading has an effect on the location of the crack nucleation site [14]. Nucleation sites in LCF tend to occur at the surface of the material and propagate inward; whereas, nucleation sites in ULCF occur within the material and propagate outward, meaning that the initial internal heterogeneity of a material carries significance in this regime. Therefore, appropriate representation of a material in ULCF requires the ability to determine homogeneity or to what extent the lack thereof will compromise the performance of the material.

5.2 Failure mode and void geometry

Multiple energy dissipation models attempted to evaluate material effects on the ULCF performance of structural steels [22, 15]. These continuous models focus on cyclic strain hardening and equate energy dissipation to damage accumulation. [17] considered ULCF as the sum of three damage modes: tensile straining, ductility exhaustion, and crack propagation, and [18] also realized that void growth and coalescence mechanisms commonly associated with ULCF failure point towards ductility exhaustion. [15] submitted that the mechanisms that lead to ductility exhaustion (like cyclic hardening and cracking) are the manifestation of microstructure evolutions, and [23] proposed that ductile crack growth is limited by initial void size and

consequential growth and micro void coalescence. Not only is the initial pore size significant in modeling, but the pore shape can change during cycling [4], a phenomenon that alters the stress state of the material throughout tension and compression phases and is the main cause of ductile fracture [14]. Although each model has pointed to the significance of pore size and distribution, none have accurately portrayed a material's intrinsic behavior in this regime.

5.3 Necessity of length scale work

Micromechanical ductile fracture models rely on assumptions regarding effective length and similitude; therefore, [14] developed a micromechanical cyclic void growth model (MM-CVGM) for ULCF based on monotonic loading which is deemed reasonable due to the similarity in failure mode; however, this model assumed micromechanical performance based on ABAQUS simulations of spherical, pre-existing voids and does not account for variances in void shape or voids that form during the cycling process. Nearly every steel contains carbides or inclusions in its lattice structure that act as void nucleation sites [4], and few studies of the fatigue behavior of SLM materials can be used to develop numeric models [5]. Therefore, a comprehensive material test is needed to understand the nature of AM steel in the absence of voids, given that initiation stems from microstructural defects [2].

5.4 Applying this work to future studies

This study establishes a baseline for the performance of AM 17-4 PH stainless steel in ULCF. Current models and simulations lack the necessary considerations to appropriately model the performance of this material; therefore, microscale tensile and ULCF tests are needed to understand the capacity of this material without inherent voids. Once the capacity is understood, models can randomly distribute imperfections until a reasonable approximation is developed. These micromechanical simulations coupled with microstructural evolution models will allow

for interchangeable, robust prediction models [4, 18, 14], from which, ε-N plots will be developed and applied to industry design.

6. References

[1] Jiangsu ROAD Damping Technology CO., Ltd., "Metallic Yield Damper," 2017. [Online]. [Accessed 24 October 2020].

[2] Yadollahi A., Shamsaei N., Thompson S.M.,Elwany A., Bian L., Mahmoudi M., "Effects of building orientation and heat treatment on fatigue behavior of selective laser melted 17-4 PH stainless steel," *International Journal of Fatigue,* pp. 218-235, 2017.

[3] Carlton H.D., Haboub A., Gallegos G.F., Parkinson D.Y., MacDowell A.A., "Damage evolution and failure mechanisms in additively manufactured stainless steel," *Materials Science & Engineering A,* pp. 406-414, 2016.

[4] Kanvinde A.M., Deierliein G.G.,"Continuum Based Micro-Models for Ultra Low Cycle Fatigue Crack Initiation in Steel Structures," in *Structures Congress 2005: Metropolis and Beyond,* 2005.

[5] Afkhami S., Dabiri M., Alavi S.H., Bjork T., Salminen A., "Fatigue characteristics of steels manufactured by selective laser melting," *International Journal of Fatigue,* pp. 72-83, 2019.

[6] Frazier W.E., "Metal additive manufacturing: a review," *Journal of Materials Engineering and performane 23.6,* pp. 1917-1928, 2014.

[7] Yadollahi A., Shamsei N., Thompson S.M., Elwany A., Bian L., Mahmoudi M., "Fatigue Behavior of Selective Laser Melted 17-4 PH Stainless Steel," in *26th International Solid Freeform Fabrication Symposium,* Austin,TX, 2015.

[8] Yadollahi A., Shamsei N., Thompson S.M., Elwany A., Bian L., Mahmoudi M., "Mechanical and Microstructural Properties of Selective Laser Melted 17-4 PH Stainless Steel," in *ASME 2015 International Mechanical Engineering Congress & Exposition,* Houston, TX, 2015.

[9] Spierings A.B., Starr T.L., Wegener K., "Fatigue performance of additive manufactured metallic parts," *Rapid Prototyping Journal,* pp. 88-94, 2013.

[10] Mahmoudi M., Elwany A., Yadollahi A., Thompson S.M., Bian L., Shamsaei N., "Mechanical properties and microstructural characterization of selective laser melted 17-4 PH stainless steel," *Rapid Prototyping Journal,* pp. 280-294, 2017.

[11] Rafi H.K., Pal D., Patil N., Starr T.L., Stucker B.E., "Microstructrure and Mechanical Behavior of 17-4 Precipitation Hardenable Steel Processed by Selective Laser Melting," *Journal of Materials Engineering and Performance,* pp. 4421-4428, 2014.

[12] LeBrun T., Nakamoto T., Horikawa K., Kobayashi H., "Effecct of retained austenite on subsequent thermal processing and resultatnt mechanical properties of selective laser melted 17-4 PH stainless steel," *Materials and Design,* pp. 44-53, 2015.

[13] Cheruvathur S., Lass E.A., Campbell C.E., "Additive manufacturing of 17-4 PH stainless steel: post-processing heat treatment to achieve unifrom reproducible microstructure," *Jom 68.3,* pp. 930-941, 2016.

[14] Khandelwal K., Kiran R., "A Micromechanical Cyclic Void Growth Model for Ultra-low Cycle Fatigue," *International Journal of Fatigue,* pp. 24-37, 2015.

[15] Liu Y.B., Li Y.D., Li S.X., Yang Z.G., Chen S.M., Hui W.J., Weng Y. Q., "Prediction of the S-N curves of high strength steels in the very high cycle fatigue regime," *International Journal of Fatigue,* pp. 1351-1357, 2010.

[16] Manson S.S., "Fatigue: a complex subject - some simple approximations.," *Experimental mechanics,* pp. 193-226, 1965.

[17] Kuroda M., "Extremely low cycle fatigue life prediction based on a new cumulative fatigue damage model," *International Journal of Fatigue,* pp. 699-703, 2001.

[18] Kaninde A.M., Deierlein G.G., "Cyclic Void Growth Model to Assess Ductile Fracture Initiation in Structural Steels due to Ultra Low Cycle Fatigue," *Journal of Engineering Mechanics,* pp. 701-712, 2007.

[19] ASTM, "ASTM Standard E 606-12 - standard practice for strain-controlled fatigue testing," 2012.

[20] Tateishi K., Hanji T., Minami K., "A prediction model for extremely low cycle fatigue strength of structural steel," *International Journal of Fatigue 29.5,* pp. 887-896, 2007.

[21] Liu R., Zhang Z.J., Zhang P., Zhang Z.F., " "Extremely-low-cycle fatigue behaviors of Cu and Cu-Al alloys: Damage mechanisms and life prediction,"," *Acta Materialia,* pp. 341-356, 2015.

[22] Nip K.H., Gardner L., Davies C.M., Elghazouli A.Y., "Extremely low cycle fatigue tests on structrual carbon and stainless steel," *Journal of Constructional Steel Research,* pp. 96-110, 2010.

[23] Tvergaard V., Hutchinson J.W., "Two mechanisms of ductile fracture: void by void growth versus multiple void interaction," *International Journal of Solids and Structrues,* pp. 3581-3597, 2002.